Available online at www.sciencedirect.com
SCIENCE DIRECT®
ELSEVIER
Bioorganic & Medicinal Chemistry 12 (2004) 113–117
Bioorganic & Medicinal Chemistry

Analogues of FAUC 73 revealing new insights into the structural requirements of nonaromatic dopamine D3 receptor agonists

Carola Lenz, Frank Boeckler, Harald Hübner and Peter Gmeiner*

Department of Medicinal Chemistry, Emil Fischer Center, Friedrich Alexander University, Schuhstraße 19, D-91052 Erlangen, Germany

Received 5 August 2003; accepted 10 October 2003

Abstract—Employing the nonaromatic D3 agonist FAUC 73 as a lead compound, the dopaminergic enynes **1a**,**b** and the diene **2** (FAUC 206) were synthesized via palladium-catalyzed cross-coupling. FAUC 206 showed remarkable D3 affinity and enhanced selectivity over D4 when compared to the lead compound. To learn more about the bioactive structure of the diene moiety, computational studies including DFT-based conformational analysis and calculations of the magnetic shielding properties were performed. The electrostatic properties of the pharmacophoric π-systems were visualized by diagnostic MEP maps.

1. Introduction

Dopamine D3 receptors being identified by Sokoloff, Schwartz and co-workers,[1] have been attributed to involvement in the etiology of different CNS disorders, such as schizophrenia, Parkinson's disease and substance abuse. As a consequence, the discovery of selective D3 agonists as well as antagonists has become an active field of research.[2] In accordance with all the catecholamine, serotonin and histamine receptor ligands described, these compounds contain a basic nitrogen and an aromatic substructure.[3] Very recently, we presented FAUC 73 as the first nonaromatic dopamine receptor agonist.[4] Within FAUC 73, a conjugated enyne serves as a bioisosteric moiety simulating the aromatic catechol substructure of dopamine (Fig. 1). FAUC 73 showed high affinity and substantial selectivity for D3 over the D2 subtype. To learn more about the structural requirements for the nonaromatic π-system, we envisioned further SAR investigations. First, we were intrigued by the question whether an H-bond donor activity of the terminal sp-hybridized CH is essential. Previous binding data of a trimethylsilyl protected precursor displayed substantial D3 binding, however we were not sure whether the silyl group was completely stable towards hydrolysis during the assay. Thus, the terminal position should be replaced by a methyl group. Besides the C-methyl derivative **1a**, the hydroxymethyl substituted enyne **1b** should be synthesized when the terminal position should be exploited to introduce a hydroxyl function simulating one of the OH-groups of the neurotransmitter. Finally, the question should be addressed whether the triple bond could be displaced by a second double bond resulting in the target compound **2** including an s-*cis* or s-*trans* positioned diene moiety as a putative catechol bioisostere.

2. Results and discussion

For the synthesis of the target compounds, we started from 1,4-cyclohexanedione acetal **3** which was transformed into the central intermediate **4** by reductive amination, hydrolysis and *O*-sulfonylation (Scheme 1).[4,5] Transformation of the vinyl triflate **4** into the enyne **1a** could not be realized when following a recently described methodology employing TMS protected propyne.[6,7] However, the palladium-catalyzed reaction could be accomplished when we used gaseous propyne[8] in a pressure vial and Cacchi's conditions [$PdCl_2(PPh_3)_2$, CuI, piperidine][9] affording the enyne **1a** in 65% yield. Using the same catalyst system, reaction of the triflate **3** with propargylic alcohol furnished the enyne **1b** in 63% yield. The diene **2** was synthesized by palladium-catalyzed coupling of the triflate **4** with vinyltributyltin when modified Stille conditions[10] involving $Pd_2(dba)_3$ and P(*o*-furyl)$_3$ led to the final product **2** in 32% yield.

Receptor binding experiments were established to evaluate the binding properties of the target compounds **1a**, **1b** and **2** in comparison to the reference FAUC 73 and

* Corresponding author. Tel.: +49-9131-852-9383; fax: +49-9131-852-2585; e-mail: gmeiner@pharmazie.uni-erlangen.de

0968-0896/$ - see front matter © 2003 Elsevier Ltd. All rights reserved.
doi:10.1016/j.bmc.2003.10.011

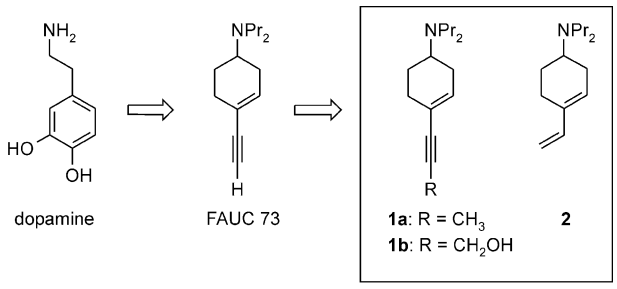

Figure 1.

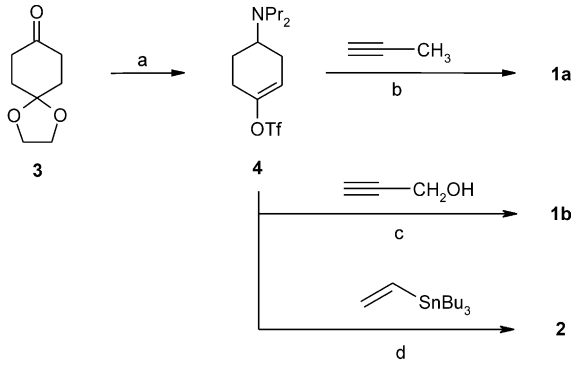

Scheme 1. Reagents and conditions: (a) (1) dipropylamine, $NaBH_3CN$, MeOH, rt, 24 h, 62%; (2) Tf_2O, 2,6-di-*tert*-butyl-4-methylpyridine, 1,2-dichloroethane, reflux, 4.5 h, 43%; (b) propyne, $PdCl_2(PPh_3)_2$, CuI, piperidine, THF, −45 °C→rt, 1.5 h, 65%; (c) propargylic alcohol, $PdCl_2(PPh_3)_2$, CuI, piperidine, THF, rt, 1 h, 63%; (d) vinyltributyltin, $Pd_2(dba)_3$, P(*o*-furyl)$_3$, NMP, rt, 3 h, 32%.

dopamine (Table 1). D1 receptor affinities were determined utilizing porcine striatal membranes and the D1 selective radioligand [^{3}H]SCH23390. D2, D3 and D4 affinities were investigated employing the cloned human dopamine receptors $D2_{long}$, $D2_{short}$,[11] D3[12] and D4.4[13] stably expressed in Chinese hamster ovary cells (CHO) and the radioligand [^{3}H]spiperone. The competition data were analyzed according to a sigmoid model by non linear regression. If the dose–response curves showed biphasic properties and the calculated Hill coefficients (n_H) were between −0.50 and −0.75 with a better fit of equation indicating a two-site model, K_i values for the high and low affinity binding sites of the receptor were derived. The $K_{i\ high}$ values representing the ternary complex of ligand, receptor and G-protein thus indicating agonist properties were compared for further SAR studies.

As observed for FAUC 73, all test compounds show only weak affinity for the D1 receptor. Formal substitution of the terminal CH of FAUC 73 by C-methyl (**1a**) or hydroxymethyl (**1b**) causes substantial reduction of D4 affinity, whereas D3 affinity depended on the size and polarity of the substituent. Thus, formal replacement of the H-atom in FAUC 73 by methyl in **1a** led only to a 10-fold decrease of D3 affinity, but introduction of a polar hydroxmethyl group strongly reduced D3 binding (K_i = 7400 nM for **1b**). Formal exchange of the triple bond by a terminal double bond led to the D3 selective agonist **2** (FAUC 206) displaying K_i values of 5.6, 230, 99, and 260 nM for D3, $D2_{long}$, $D2_{short}$ and D4, respectively. It is interesting to note, that FAUC 206 displayed a binding profile that closely resembled that of the enyne FAUC 73, however, the selectivity over D4 was improved by a factor of approximately 11 (K_i (D4:D3) = 4.2 for FAUC 73, K_i (D4:D3) = 46 for FAUC 206).

Due to the finding that not only an enyne but also a diene moiety can efficiently simulate the aromatic substructure of dopamine, we tried to characterize the structure of the diene **2** in comparison to the lead compound FAUC 73. Thus, conformational properties including the consequences on magnetic shielding and molecular electrostatic potential maps were calculated. Initially, we performed a semiempirical AM1 optimization with VAMP[14] on the s-*trans* conformer, followed by two steps of DFT calculations in Gaussian98.[15] We used a B3LYP density functional with a 3-21G basis set in order to produce a reasonable geometry in appropriate time. Then, we increased the basis set to the double-valence level 6-31G(d) to enhance the quality of the structure. At the same level, we accomplished a grid calculation varying the dihedral angle $\Phi_{1\text{-}2\text{-}3\text{-}4}$ in steps of 10°. With this dihedral frozen, the rest of the system was allowed to freely adapt to the new geometry by minimization of energy. As depicted in Figure 2, we obtained two s-*cis*-like local minima (further called 'sc1' and 'sc2') and one s-*trans*-like local minimum ('st') separated by a rotational barrier of at least 3.59 kcal/mol for sc1, 3.88 kcal/mol for sc2 and 6.89 kcal/mol for st, respectively.

Table 1. Receptor binding data for **1a**, **1b**, **2**, FAUC 73 and dopamine employing porcine D1 as well as human $D2_{long}$, $D2_{short}$, D3 and D4.4 receptors[a]

Compd	K_i values (nM)				
	[^{3}H]SCH23390		[^{3}H]spiperone		
	pD1	$hD2_{long}$	$hD2_{short}$	hD3	hD4.4
1a	44,000	110 + 16,000[b]	15,000	53 + 2600[b]	4100
1b	38,000	16,000	17,000	7400	2200
2	40,000	230 + 12,000[b]	99 + 6400[b]	5.6 + 430[b]	260 + 3100[b]
FAUC 73	49,000[c]	270 + 14,000[b]	250 + 12,000[b]	5.2 + 590[b]	22 + 380[b]
Dopamine	7 + 650[b,c]	20 + 1900[b]	17 + 1100[b]	50 + 1600[b]	1.2 + 62[b]

[a] K_i values are the means of four experiments each done in triplicate.
[b] $K_{i\ high}$ and $K_{i\ low}$ values derived from a biphasic curve, if data analysis fits better with the equations for a two-site binding mode.
[c] D1 affinity determined with bovine striatum.

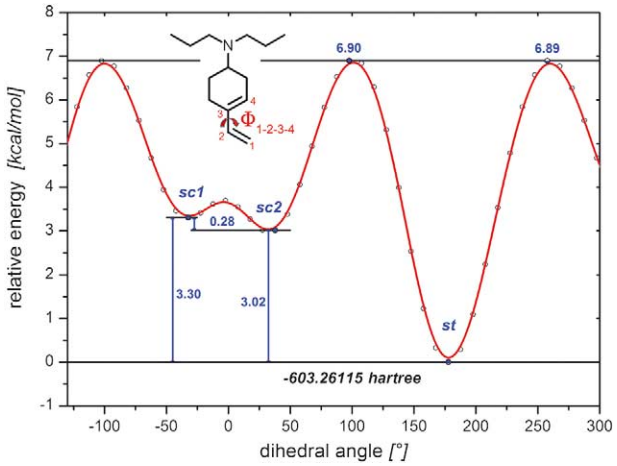

Figure 2. DFT grid-calculation of the rotational barriers and minima of the diene **2** with B3LYP/6-31G(d). For better readability the relative energies in kcal/mol applied to the lowest energy calculated (−603.26115 hartree) are denoted.

Table 2. Energy differences [kcal/mol] of the local minima

Density functional/basis set	$\Delta E_{sc2\text{-}sc1}$	$\Delta E_{st\text{-}sc2}$	$\Delta E_{st\text{-}sc1}$
B3LYP/6-311G(d)[a]	−0.32	−2.87	−3.19
B3PW91/6-311G(d)[b]	−0.34	−2.87	−3.21
B3LYP/6-311G(d,p)[a]	−0.34	−2.89	−3.23
B3PW91/6-311 + G(2d,p)[b]	−0.37	−2.94	−3.31
B3LYP/6-311 + G(2df,2p)[a]	−0.35	−3.01	−3.35
B3PW91/6-311 + G(2df,2p)[b]	−0.37	−2.99	−3.35

[a] Full optimisation.
[b] Single point calculation on previously minimized structure.

All three conformers were subjected to a series of subsequent energy minimizations with increasing basis sets using the density functionals B3LYP and B3PW91 to further improve the quality of the predictions. Therefore we enlarged our basis set to the triple-valence level, subsequently applying additional diffuse and polarization functions (Table 2). The calculations were found to give a highly consistent ranking of the conformers with almost identical relative energy differences. A small energy gap of 0.32–0.37 kcal/mol in favor of sc2 compared to sc1 was found as well as a larger gap of 2.87–3.01 kcal/mol for st compared to sc2 and 3.19 to 3.35 kcal/mol for st compared to sc1, respectively. According to the Boltzmann equation, the ratio of structures in the sc1- and st-conformation at room temperature (298.15 K) is about 0.5% and the ratio sc2/st is 0.8%, indicating that the most relevant structure for the bioactive conformation is s-*trans*.

Additionally, the structure of the transition state of the rotation around $\Phi_{1\text{-}2\text{-}3\text{-}4}$ was calculated at the 6-311G(d) level of theory. The fact that a real transition state was found was verified by frequency calculation, which yielded only one negative frequency corresponding to the examined rotational motion. The energy of the transition state was found to be 3.20 kcal/mol higher than the sc1-state, 3.52 kcal/mol higher than the sc2-state and 6.39 kcal/mol higher than the st-state demonstrating that a considerably high rotational barrier exists between the s-*cis*-like states and the s-*trans*-like state.

To gain further evidences for the bioactive conformation, we calculated the magnetic shielding tensor using gauge invariant atomic orbitals[16] (GIAO) within a B3PW91/6-311 + G(2d,p) or B3PW91/6-311 + G(2df,2p) single point calculation. The chemical shifts for all olefinic protons (A, B, C and D as depicted in Fig. 3) were calculated by subtraction of the total shielding (average isotropic value) of the respective proton from the total shielding of a TMS-proton:

$$\delta_{x\in\{A,B,C,D\}} = \sigma_{TMS} - \sigma_x;$$

TMS as a reference was optimized and subjected to NMR single point calculations on the same levels as the compared structures utilizing its T_d-symmetry. The chemical shifts were obtained with an average deviation from experimental values of 0.31 ppm for the s-*cis*-like and 0.26 ppm for the s-*trans*-like structures at the 6-311 + G(2d,p)-level as well as 0.38 ppm for the s-*cis*-like and 0.32 ppm for the s-trans-like structures at the 6-311 + G(2df,2p)-level. What is more, the comparison of similar and dissimilar olefinic protons revealed marked differences between sc1/sc2 and st. While the chemical shifts for H^A and H^B in the s-*cis*-like structures are separated by 0.42 to 0.56 ppm, in the s-*trans* structure the separation is only 0.08 or 0.16 ppm, respectively, which is in very good agreement with the experimental value (Table 3). Likewise, the difference of the chemical shifts for H^C and H^D is found to be quite low, with only 0.20–0.27 ppm in the s-*cis*-like structures, whereas in the s-*trans* structure the difference again is almost identical with the experimental data (0.63/0.72 ppm compared to 0.68 ppm). Renouncing effects of the receptor binding cavity, >99% of the substance should be in the s-*trans*-state.

In order to understand the structural requirements for receptor recognition, we decided to take a closer look at the molecular electrostatic potentials (MEPs). The diene **2** and the enyne FAUC 73 were pre-optimized with B3LYP/3-21G and subsequently optimized with B3LYP/6-311G(d). The charges used to contour the MEPs were calculated on the resulting structures applying Breneman's CHelpG charge distribution scheme. The positive and negative isopotential surfaces were contoured with MOLCAD Plus implemented in Sybyl 6.9.1[17] at +2.0 or −2.0 kcal/mol, respectively. The negative electrostatic potential surrounding the enyne substructure in FAUC 73 and upside and downside of the diene **2** (FAZC 206) shows significant shape similarity (Fig. 4). As previously suggested for FAUC 73, this structural feature obviously mimics the aromatic moiety of dopamine.

In conclusion, SAR studies showed that substitution of the acetylene proton of FAUC 73 could possibly destroy H-bond-like interactions, for example with the serine residues in TM5. Taking into account, however, that the diene **2** also lacks a proton of similar chemical characteristics, but binds to the D3 receptor with high affinity, the hypothesis that the acetylene proton is of pharmacophoric importance seems to be unlikely. Computational studies demonstrate that the s-*trans*-conformer of

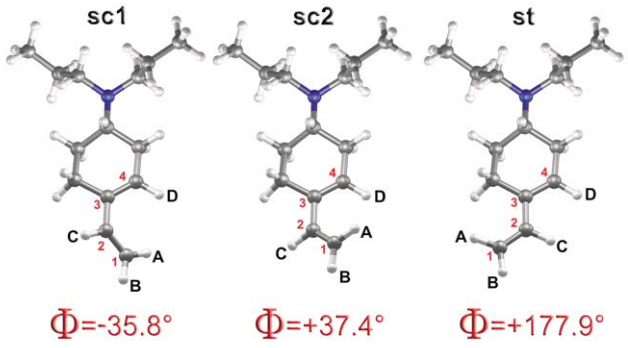

Figure 3. Final geometries obtained for B3LYP/6-311 + G(2df,2p) with the dihedral angle Φ and the labeling of the olefinic protons as used in ^{1}H NMR calculations (see Table 3).

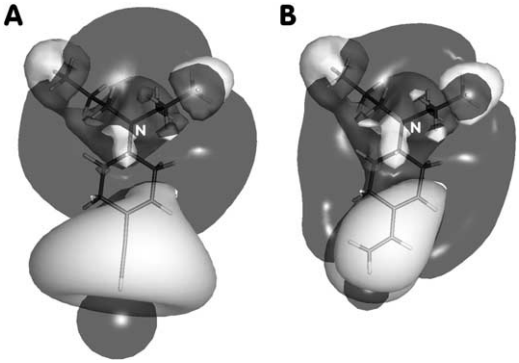

Figure 4. Isopotential surfaces of FAUC 73 (A) and the diene **2** (B) contouring positive (dark grey, + 2 kcal/mol) and negative (light grey, −2 kcal/mol) electrostatic potentials.

Table 3. Differences in chemical shifts (ppm)

	B3PW91/6-311 + G(2d,p)		B3PW91/6-311 + G(2df,2p)	
	$\delta(H^A)-\delta(H^B)$	$\delta(H^C)-\delta(H^D)$	$\delta(H^A)-\delta(H^B)$	$\delta(H^C)-\delta(H^D)$
sc1	0.51	0.23	0.51	0.20
sc2	0.56	0.27	0.42	0.25
st	0.16	0.63	0.08	0.72
Exp.	**0.13**	**0.68**	**0.13**	**0.68**

the diene **2** (FAUC 206) is expected to interact with the receptor. In this case, the relative orientation of the conjugated π-system is obviously similar to the orientation of the aromatic moiety in dopamine being necessary to form favorable interactions with aromatic residues putatively in TM6 of the receptor.

3. Experimental

Reactions were performed under dry N_2. Solvents were purified and dried under standard procedures. All reagents were of commercial quality and used as purchased. Flash chromatography was carried out with silica gel 60 (4.0–6.3 μm) eluting with an appropriate solvent in the stated v/v proportions. ^{1}H and ^{13}C NMR spectra were obtained in $CDCl_3$ on Bruker AM 360 (360 MHz) and Bruker AC 250 (90 MHz) spectrometers, respectively. MS and HRMS were run on Finnigan MAT TSQ 70 and 8200 spectrometers, respectively, by EI (70 eV). IR spectra were recorded on a Jasco FT/IR 410 spectrometer. All quantum chemical calculations were performed on a four-nodes Linux Cluster consisting of 2 Intel Xeon 2.6 GHz processors each and running SuSE linux 8.1. Visualization of molecular electrostatic potentials was prepared on a SGI Octane2.

3.1. Dipropyl[4-(prop-1-yn-1-yl)cyclohex-3-en-1-yl]amine (1a)

To a suspension of $PdCl_2(PPh_3)_2$ (10 mg, 0.014 mmol) and CuI (4 mg, 0.023 mmol) in THF (3.5 mL) in a pressure vial were added a solution of **4** (47 mg, 0.14 mmol) in THF (0.5 mL) and piperidine (70 μL, 0.7 mmol) and the mixture was cooled to −45 °C. After bubbling propyne through the solution for 30 min, the vial was sealed and the mixture was stirred for 1.5 h at room temperature. After cooling to −45 °C again, saturated aqueous $NaHCO_3$ solution was added and the aqueous layer was extracted with EtOAc. The combined organic layers were dried ($MgSO_4$) and evaporated. The residue was purified by flash chromatography (CH_2Cl_2–MeOH–MeOH satd with NH_3 95:5:1) to give **1a** as a slightly yellowish oil (20 mg, 65%): IR (film) 2956, 2873, 2225, 1635, 1462, 1271, 1029 cm^{-1}; ^{1}H NMR δ 0.86 (t, J = 7.6 Hz, 6H, 2× $NCH_2CH_2C\underline{H}_3$), 1.39–1.49 (m, 5H, 2× $NCH_2C\underline{H}_2CH_3$, 6-$H_{ax}$), 1.81–1.88 (m, 1H, 6-$H_{eq}$), 1.92 (s, 3H, C≡C–$CH_3$), 2.01–2.10 (m, 1H, 2-H or 5-H), 2.16–2.22 (m, 3H, 2-H, 5-H), 2.43–2.48 (m, 4H, 2× $NC\underline{H}_2CH_2CH_3$), 2.76 (dddd, J = 12.4, 10.3, 5.0, 2.6 Hz, 1H, 1-H_{ax}), 5.94–5.96 (m, 1H, 3-H); EIMS 219 (M^+); HREIMS (M^+) 219.1985 (219.1987 calcd for $C_{15}H_{25}N$).

3.2. 3-[4-(Dipropylamino)cyclohex-1-en-1-yl]prop-2-yn-1-ol (1b)

To $PdCl_2(PPh_3)_2$ (11 mg, 0.015 mmol) and CuI (4 mg, 0.023 mmol) in THF (2 mL) were added a solution of **4** (50 mg, 0.15 mmol) in THF (0.5 mL), propargylic alcohol (35 μL, 0.6 mmol) and piperidine (75 μL, 0.76 mmol). After being stirred at room temperature for 1 h, saturated aqueous $NaHCO_3$ solution was added and the aqueous layer was extracted with EtOAc. The combined organic layers were dried ($MgSO_4$) and evaporated. The

residue was purified by flash chromatography (CH_2Cl_2–MeOH–MeOH satd with NH_3 9:1:1) to give **1b** as a slightly yellowish oil (22 mg, 63%): IR (film) 3347, 2958, 2871, 2215, 1666, 1457, 1203, 1024 cm^{-1}; ^1H NMR δ 0.87 (t, $J = 7.5$ Hz, 6H, 2× $NCH_2CH_2C\underline{H}_3$), 1.39–1.53 (m, 5H, 2× $NCH_2C\underline{H}_2CH_3$, 5-$H_{ax}$), 1.86 (dddd, $J = 9.4$, 7.5, 4.9, 2.8 Hz, 1H, 5-H_{eq}), 1.87–1.91 (brs, 1H, $CH_2O\underline{H}$), 2.04–2.13 (m, 1H, 3-H or 6-H), 2.19–2.28 (m, 3H, 3-H, 6-H), 2.37–2.44 (m, 4H, 2× $NC\underline{H}_2CH_2CH_3$), 2.76 (dddd, $J = 12.0$, 10.7, 4.9, 2.8 Hz, 1H, 4-H_{ax}), 4.36 (s, 2H, $C\underline{H}_2OH$), 6.05–6.08 (m, 1H, 2-H); ^{13}C NMR δ 11.8 ($NCH_2CH_2\underline{C}H_3$), 21.8 ($NCH_2\underline{C}H_2CH_3$), 25.0 (C-5), 28.4, 30.2 (C-3, C-6), 51.5 (CH_2OH), 52.6 ($N\underline{C}H_2CH_2CH_3$), 55.6 (C-4), 85.0, 86.8 (C≡C), 120.0 (C-2), 134.6 (C-1); EIMS 235 (M^+); HREIMS (M^+) 235.1933 (235.1936 calcd for $C_{15}H_{25}NO$).

3.3. Dipropyl(4-vinylcylohex-3-en-1-yl)amine (2)

To a solution of **4** (20 mg, 0.06 mmol) in NMP (1 mL), $Pd_2(dba)_3$ (1.6 mg, 0.002 mmol) and P(*o*-furyl)$_3$ (2.5 mg, 0.012 mmol) were added. After being stirred for 10 min at room temperature, vinyltributyltin (25 μL, 0.09 mmol) was added and stirring was continued for 3 h. After that saturated aqueous $NaHCO_3$ solution was added and the aqueous layer was extracted with Et_2O. The combined organic layers were dried ($MgSO_4$) and evaporated. The residue was purified by flash chromatography over basic alumina oxide (CH_2Cl_2–MeOH 99:1) to give **2** as a colourless oil (4 mg, 32%): IR (film) 2957, 2872, 1644, 1607, 1463, 1378, 1078, 892 cm^{-1}; ^1H NMR δ 0.87 (t, $J = 7.5$ Hz, 6H, 2× $NCH_2CH_2C\underline{H}_3$), 1.39–1.50 (m, 5H, 2× $NCH_2C\underline{H}_2CH_3$, 6-H), 1.90–1.96 (m, 1H, 6-H), 2.02–2.26 (m, 3H, 2-H, 5-H), 2.34–2.47 (m, 5H, 2× $NC\underline{H}_2CH_2CH_3$, 2-H or 5-H), 2.79 (dddd, $J = 12.2$, 10.1, 5.2, 2.6 Hz, 1H, 1-H_{ax}), 4.91 (d, $J = 10.8$ Hz, 1H, C=CH_2), 5.04 (d, $J = 17.5$ Hz, 1H, C=CH_2), 5.71–5.73 (m, 1H, 3-H), 6.34 (dd, $J = 17.5$, 10.8 Hz, 1H, $\underline{H}C$=CH_2); EIMS 207 (M^+); HREIMS (M^+) 207.1989 (207.1987 calcd for $C_{14}H_{25}N$).

3.4. Receptor binding experiments and data analysis

Receptor binding studies were carried out as described in literature.[4] In brief, the dopamine D1 receptor assay was done with porcine striatal membranes at a final protein concentration of 40 μg/assay tube and the radioligand [^{3}H]SCH23390 at 0.3 nM ($K_d = 0.7$–1.1 nM). Competition experiments with the human $D2_{long}$, $D2_{short}$, D3 and D4.4 receptors were run with preparations of membranes from CHO cells expressing the corresponding receptor and [^{3}H]spiperone at a final concentration of 0.1 nM. The assays were carried out at a protein concentration of 3–30 μg/assay tube and K_d values of 0.10 nM for $D2_{long}$ and $D2_{short}$, 0.10–0.30 nM for D3 and 0.39–0.98 nM for D4.4.

The resulting competition curves were analyzed by nonlinear regression using the algorithms in PRISM (GraphPad Software, San Diego, USA). The data were initially fit using a sigmoid model to provide a slope coefficient (n_H) and an IC_{50} value, representing the concentration corresponding to 50% of maximal inhibition. Data were then calculated for a one-site ($n_H \sim 1$) or a two-site model ($n_H < 1$) depending on the slope factor. IC_{50} values were transformed to K_i values according to the equation of Cheng and Prusoff.[18]

Acknowledgements

The authors wish to thank Dr. H. H. M. Van Tol (Clarke Institute of Psychiatry, Toronto, Canada), Dr. J.-C. Schwartz, and Dr. P. Sokoloff (INSERM, Paris, France) as well as J. Shine (The Garvan Institute of Medical Research, Sydney, Australia) for providing dopamine D4, D3, and D2 receptor expressing cell lines, respectively. Thanks are also due to Mrs. Jung, Mrs. Schmitt and Mrs. Szczepanek for skillful technical assistance. This work was supported by the BMBF and Fonds der Chemischen Industrie.

References and notes

1. Sokoloff, P.; Giros, B.; Martres, M.-P.; Bouthenet, M.-L.; Schwartz, J.-C. *Nature* **1990**, *347*, 146.
2. Luedtke, R. R.; Mach, R. H. *Curr. Pharm. Des.* **2003**, *9*, 643.
3. Crider, A. M.; Scheideler, M. A. *Mini Rev. Med. Chem.* **2001**, *1*, 89.
4. Hübner, H.; Haubmann, C.; Utz, W.; Gmeiner, P. *J. Med. Chem.* **2000**, *43*, 756.
5. Demopoulos, V. J.; Gavalas, A.; Rekatas, G.; Tani, E. *J. Heterocycl. Chem.* **1995**, *32*, 1145.
6. Halbes, U.; Bertus, P.; Pale, P. *Tetrahedron Lett.* **2001**, *42*, 8641.
7. Bertus, P.; Halbes, U.; Pale, P. *Eur. J. Org. Chem.* **2001**, 4391.
8. Zhang, Q.; Shi, C.; Zhang, H.-R.; Wang, K. K. *J. Org. Chem.* **2000**, *65*, 7977.
9. Cacchi, S.; Morera, E.; Ortar, G. *Synthesis* **1986**, 320.
10. Farina, V.; Krishnan, B. *J. Am. Chem. Soc.* **1991**, *113*, 9585.
11. Hayes, G.; Biden, T. J.; Selbie, L. A.; Shine, J. *Mol. Endocrinol.* **1992**, *6*, 920.
12. Sokoloff, P.; Andrieux, M.; Besancon, R.; Pilon, C.; Martres, M.-P.; Giros, B.; Schwartz, J.-C. *Eur. J. Pharmacol.* **1992**, *225*, 331.
13. Asghari, V.; Sanyal, S.; Buchwaldt, S.; Paterson, A.; Jovanovic, V.; Van Tol, H. H. M. *J. Neurochem.* **1995**, *65*, 1157.
14. Clark, T.; Alex, A.; Beck, B.; Chandrasekar, J. et al. *Program Package VAMP 7.0*; Oxford Molecular Group: Oxford, 1998.
15. Frisch, M. J.; Trucks, G. W.; Schlegel, H. B.; Scuseria, G. E. *Gaussian 98*, Revision A.7; Gaussian: Pittsburgh, PA, 1998.
16. Wolinski, K.; Hinton, J. F.; Pulay, P. *J. Am. Chem. Soc.* **1990**, *112*, 8251.
17. *SYBYL 6.9.1*, Tripos: 1699 South Hanley Rd., St. Louis, MO, 63144, USA.
18. Cheng, Y. C.; Prusoff, W. H. *Biochem. Pharmacol.* **1973**, *22*, 3099.